

Coupled-Cavity Lasers for a Low-Power Integrated Coherent Optical Receiver

Shamsul Arafin¹, Gordon Morrison², Milan Mashanovitch², Leif A. Johansson², and Larry A. Coldren¹

¹Department of Electrical and Computer Engineering, University of California, Santa Barbara, CA, 93106, USA.

²Freedom Photonics LLC, Santa Barbara, CA, 93117, USA

sarafin@ece.ucsb.edu

Abstract: Compact, tunable, low-power consumption coupled-cavity lasers are designed and experimentally demonstrated. Single-mode operation with an SMSR >24 dB and >11 nm tuning range are achieved, being suitable as on-chip local oscillators in low-power integrated optical coherent receivers.

OCIS codes: (140.3600) Lasers, tunable; (130.3120) Integrated optics devices.

In InP-based integrated coherent optical receivers, tunable lasers are one of the major components which consume most of the electrical power. In order to reduce the power consumption in the PICs, it is currently of significant interest to explore advanced designs of low-power, widely-tunable lasers. Among such designs, Y-branch [1] and simple co-linear coupled-cavity (C-C) lasers were found to be possible ways by which the present and future power requirements might be accommodated. Coupled-cavity design using grating bursts as intercavity coupling elements is proposed here. Although the operating principle as well as some analysis of this kind of laser was reported in the 1980's [2-3], the recent work has been more focused on the low-power consumption and wide tuning-range specifications. Furthermore, due to their potentially short cavities, high fill-factors for the gain regions, and compatibility with PIC fabrication processes, the C-C designs could be more efficient, compared to matured- and low-risk widely tunable lasers, e.g. sampled-grating distributed Bragg reflector (SG-DBR).

A theoretical study of C-C lasers was performed. Figure 1(a) shows an example schematic view of a multi-section C-C laser using an active-passive scheme. It consists of two cavities, denoted as cavity-1 and cavity-2, and each can have active and passive regions isolated by proton implants. In this case, cavity-1 is formed by independent and electrically-isolated active and passive sections whose geometrical lengths are 90 μm and 40 μm , respectively. Similarly, cavity-2 consists of an independent 150- μm -long active section.

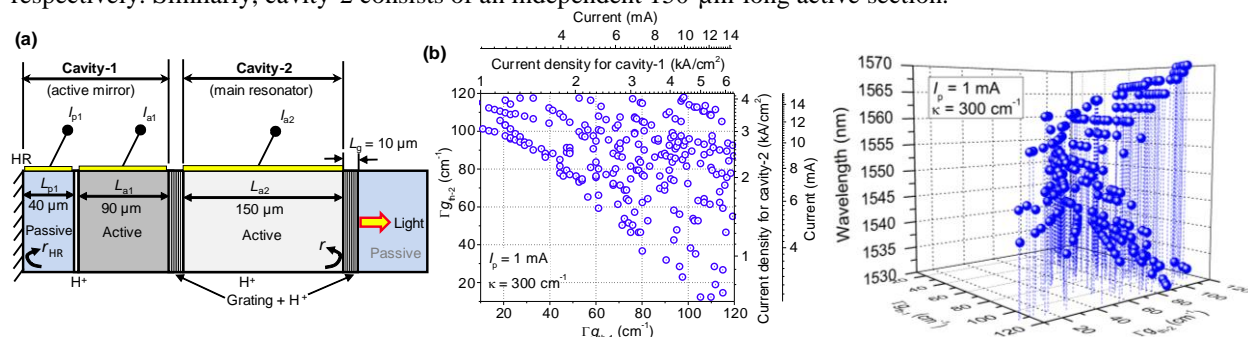


Fig. 1: (a) Schematic illustration of a coupled-cavity laser with three electrodes. The rightmost-long section labeled by “Passive” is not a part of the resonator, (b) 2D plot for modal threshold gain, $\Gamma_{\text{th},1}$ vs $\Gamma_{\text{th},2}$ and corresponding current densities for the lasing modes, where phase current is fixed, and (c) 3D trajectories, showing modal threshold gain, $\Gamma_{\text{th},1}$ vs $\Gamma_{\text{th},2}$ and corresponding resonant wavelengths as a third dimension. The intra-cavity grating mirror coupling constant, κ was fixed at a relatively weak value of 300 cm^{-1} .

Although the C-C system laser as one resonator, one can gain some intuitive understanding of its operation by thinking of it as two Fabry- P erot cavities, each with their own mode spacings that interfere to reinforce one mode of the coupled system, as in a Moorea pattern or a Vernier scale. In this example, the mode spacing for cavity-1 and cavity-2 is calculated to be 2.4 nm and 2.1 nm, respectively, resulting a spacing mismatch of 0.3 nm and a possible repeat mode every 16.8 nm. The phase tuning sections enable the modes to be tuned continuously.

The interference or the coupling between cavity-1 and cavity-2 is mainly determined by the reflectivities of the mirrors present in the resonator. In this case, strong reflection ($r_{\text{HR}} \approx 0.95$) from the HR coating at the left side and weak reflections ($r_{\text{grating}} \approx 0.3$) from each of the gratings in the resonator influences the coupling between these two cavities. The grating reflection is relatively weak using present design rules ($\kappa = 300 \text{ cm}^{-1}$) and a length (10 μm) that will enable a reasonable tuning range of ~ 30 nm. The phase section may be longer than necessary to get the needed net π -phase shift. Configurations with shorter phase sections as well as different cavity lengths are being investigated.

The modal threshold gain and the lasing wavelength can be calculated by observing the net transfer function, S_{21} , across the entire device from the HR mirror to the right-most grating. In a numerical calculation, the transmission

spectrum of S_{21} for the coupled system will develop a strong maximum at some wavelength, as the gain is increased through electrical pumping. The gain values required for this maximum to reach some large value and its wavelength are the desired threshold values. In other words, the poles of S_{21} for the entire system provide the pair of modal threshold gains for the cavities and the resonant wavelength values $\lambda_{\text{resonant}}$. The phase currents are dithered to optimize the modal selectivity with a reasonably good side-mode suppression-ratio (SMSR).

Figure 1(b) gives threshold modal gain pair solutions for wavelengths ranging from 1535 nm to 1575 nm. A 2D plot of the threshold modal gain of cavity-1, $\Gamma_{g_{\text{th-1}}}$, versus the threshold modal gain of cavity-2, $\Gamma_{g_{\text{th-2}}}$, together with the corresponding current and current densities required to reach threshold assuming a fixed phase current in the passive section is shown here. The data is obtained by fixing $\Gamma_{g_{\text{th-1}}}$ and solving for $\Gamma_{g_{\text{th-2}}}$ and $\lambda_{\text{resonant}}$ for each given $\Gamma_{g_{\text{th-1}}}$ over a prescribed range of wavelengths. Then, $\Gamma_{g_{\text{th-1}}}$ is increased and the process repeated. It should be noted that $\Gamma_{g_{\text{th-1}}}$ is determined by the applied current into the gain section of cavity-1, where the confinement factor is $\Gamma = 0.1$. Gain parameters are obtained from [4]. 3D trajectories is shown in Fig. 1(c), where wavelength is included as a third dimension, illustrating $\lambda_{\text{resonant}}$ that cover the entire range between 1535 nm and 1575 nm for the realistic condition, $\Gamma_{g_{\text{th}}} < 120 \text{ cm}^{-1}$. The missing wavelength values in Fig. 1(c) can be filled out by changing the phase current independently in phase sections of cavity-1 and cavity-2.

Lasers were fabricated in a PIC platform where an offset quantum well (OQW) integration technique was employed [5]. The multi-quantum well (MQW) region acts as the gain medium for the laser device as well as a semiconductor optical amplifier (SOA) that was integrated after the laser. A microscope picture of the fully-processed PIC with a C-C laser and SOA is shown in Fig. 2(a). For testing, devices were mounted on a ceramic carrier and wire bonded, as shown in Fig. 2(a).

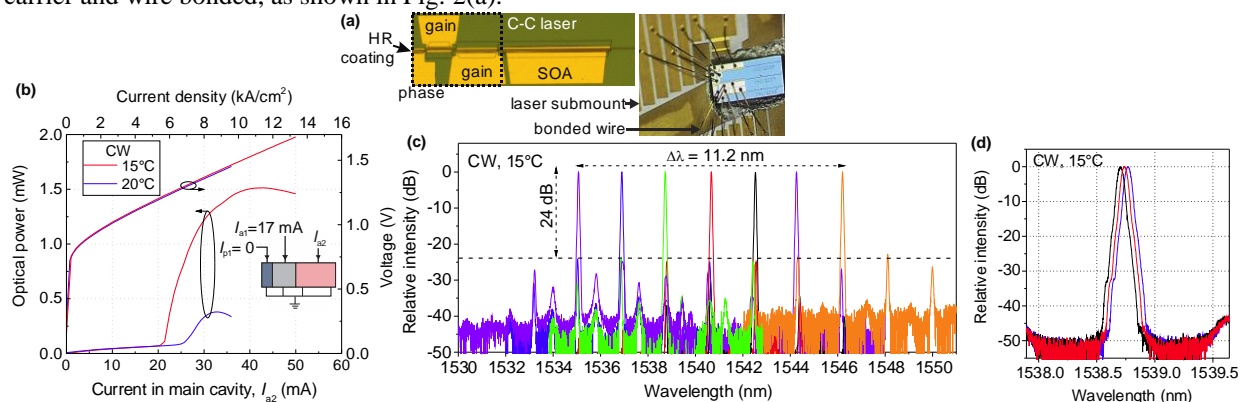


Fig. 2 (a) Microscope image of processed C-C laser with SOA=semiconductor optical amplifier, and microscope image of C-C laser chip mounted on the carrier and wirebonded, (b) measured light-current-voltage characteristics of C-C lasers as a function of temperature, (c) spectra of the laser by varying current in cavity-1 and cavity-2, and (d) fine tuning of the emission wavelength by changing current in the phase section.

Temperature dependent continuous-wave (CW) light-current-voltage ($L-I-V$) characteristics of devices were measured on a Peltier-cooled copper heatsink, as displayed in Fig. 2(b). The device shows CW operation up to room-temperature. Measurements were performed when the current in cavity-1 is fixed to 17 mA and no current in the phase section is applied. On-chip SOA, reverse biased by 2 V, was used as a photodetector with an assumed responsivity of 1 A/W to measure the optical power coming out from the device.

The emission spectra of the C-C device are shown in Fig. 2(c), which was obtained by varying the current in cavity-1 and cavity-2 and keeping the current in the phase section constant. The single-frequency wavelength tuning range of such devices is measured to be 11.2 nm. The device exhibits single-mode operation over this entire operating range with an SMSR >24 dB. Use of higher κ -gratings [6] should enable improved SMSR as well as wider tuning ranges and lower threshold currents. The fine tuning of the emission wavelength (Fig. 2(d)) was measured by varying the phase-section current at a constant current in both cavities, yielding mode-hop-free tuning range of ~ 0.07 nm. In addition to these static properties of such C-C devices, the potential of such devices in coherent receiver PICs will also be reported at the conference.

[1] J.-O. Wesström, et al., "State of the art performance of widely tunable modulated grating Y-branch lasers," in Proc. OFC, paper TuE2 (2004).

[2] L. B. Allen, H. G. Koenig, and R. R. Rice, "Single Frequency Injection Laser Diodes for Integrated Optics and Fiber Optics Applications", Proc. Soc. Photo. Opt. Eng. **157**, 110-117 (1978).

[3] L. A. Coldren, and T. L. Koch, "Analysis and design of coupled-cavity lasers - Part I: Threshold gain analysis and design guidelines", IEEE J. Quantum Electron. **20**, 659 – 670 (1984).

[4] L. A. Coldren, S. W. Corzine, and M. L. Mashanovich, *Diode Lasers and Photonic Integrated Circuits* (Wiley, New York, 2012), Chap. 4.

[5] J.W. Raring, et al., "Advanced integration schemes for high-functionality/high-performance photonic integrated circuits", Proc. SPIE **6126**, 61260H (2006).

[6] C.H. Chen, et al., "Compact Beam Splitters with Deep Gratings for Miniature Photonic Integrated Circuits: Design and Implementation Aspects", Appl. Opt. **48**, F68-F75 (2009).